JOURNAL OF THE AMERICAN CHEMICAL SOCIETY

Communication

pubs.acs.org/JACS

Splitting Molecular Oxygen en Route to a Stable Molecule Containing Diphosphorus Tetroxide

Yuzhong Wang, Yaoming Xie, Pingrong Wei, Henry F. Schaefer, III, Paul von R. Schleyer, and Gregory H. Robinson*

Department of Chemistry and the Center of Computational Chemistry, The University of Georgia, Athens, Georgia 30602-2556, United States

Supporting Information

ABSTRACT: In contrast to stable phosphorus oxides such as P_4O_6 and P_4O_{10} that possess iconic adamantane-like cage structures, highly reactive phosphorus oxides such as PO, PO_2, and P_2O_x ($x = 1-5$) only have been studied in the gas phase or by matrix isolation techniques. Elusive diphosphorus tetroxide, the long sought phosphorus analogue of N_2O_4, is particularly noteworthy. Computations predict that the oxo-bridged O_2POPO form of P_2O_4 is energetically more favored than the P−P bonded O_2P-PO_2 isomer. Herein, we report the experimental realization of diphosphorus tetroxide—in its energetically disfavored O_2P-PO_2 form—via carbene-stabilization. The synthesis of the title compound involves the splitting of molecular oxygen by carbene-stabilized diphosphorus.

The Periodic Table suggests that elements in the same group generally exhibit similar chemical properties. Although phosphorus resides immediately beneath nitrogen on the Periodic Table, the chemical behavior of these two elements is quite different. This disparity is not only evident for the elements, but it also extends to the compounds of these first two pnictogens.[1] For example, nitrogen gas (N_2) is both tremendously stable and ubiquitous (making up nearly 80% of the earth's atmosphere). In contrast, diphosphorus (P_2) is transient and generally only observed at high temperatures.[1] Furthermore, nitrogen readily forms a series of *isolable* oxides, (such as NO, NO_2, N_2O_x (x = 1, 3, 4, 5)) that have had a profound impact on both our environment and various aspects of the human experience.[2] The stable oxides of phosphorus, such as P_4O_6 and P_4O_{10}, contain iconic adamantane-like cores.[1] However, the phosphorus congeners of those isolable nitrogen oxides [i.e., PO, PO_2, P_2O_x (x = 1, 3, 4, 5)] are highly reactive and typically only studied in the gas phase or in matrix isolation experiments at cryogenic temperatures.[3] Consequently, synthetic applications of these reactive phosphorus oxides are severely limited.

The first transition metal compounds containing phosphorus monoxide (PO) and diphosphorus monoxide (P_2O) were reported more than two decades ago.[4,5] However, alternative synthetic strategies are imperative to develop the largely unexplored chemistry of these extremely reactive phosphorus oxides. In this regard, diphosphorus tetroxide, P_2O_4, is particularly intriguing. Computations suggest that P_2O_4 energetically favors an oxo-bridged, nonplanar O_2POPO structure (with C_s symmetry), rather than its O_2P-PO_2 isomer.[6,7] In contrast, dinitrogen tetroxide (N_2O_4) exists as a weakly N−N-bonded O_2N-NO_2 dimer.[1] Whether P_2O_4 can be stabilized as an analogue of N_2O_4 (in the O_2P-PO_2 form) clearly represents a fascinating synthetic challenge. Carbene-stabilization has recently emerged as a remarkably effective synthetic strategy in the isolation of highly reactive, low-oxidation state, main group molecules.[8−13] This laboratory previously reported the synthesis of carbene-stabilized diphosphorus, L:P−P:L, (L: = N-heterocyclic carbene; :C{N-(2,6-$Pr^i_2C_6H_3$)CH}$_2$) (**2**)[14] by potassium graphite reduction of L:PCl_3 (**1**).[15] Herein, we report the synthesis,[16] molecular structure,[16] and computational analysis[17] of carbene-stabilized diphosphorus tetroxide L:$(O)_2P-P(O)_2$:L (**3**), which is obtained via the splitting of molecular oxygen by compound **2**. Phosphorus oxides are well documented as Lewis bases bonding to transition metals[18,19] or main group elements.[20,21] Notably, compound **3** represents the first example of a phosphorus oxide exhibiting Lewis acidic behavior.

Transition metal complexes have long dominated the chemistry of dioxygen binding and activation due to their critical role in oxygenation in various biological systems.[22] However, electron-rich main group species may also activate triplet O_2 molecules. For instance, autoxidation mechanisms have been proposed in the transformation of phosphanylidenephosphoranes (RP═PR_3) into diphosphenes.[23] The synthesis of long-pursued sila-ureas, via silicon(II)-based dioxygen activation, has also been reported.[24] Inspired by the classic oxidation of white phosphorus to P_4O_{10},[1] we allowed (red-colored) **2** to react with dioxygen in toluene [at temperatures ranging from −6 °C to room temperature (25 °C)], giving compound **3** in 54% yield (Scheme 1). Although the

Scheme 1. Synthesis of compound 3

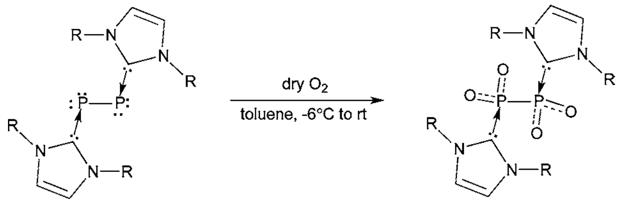

2

3

Received: November 15, 2013
Published: December 3, 2013

mechanistic details in the formation of **3** are unclear, the splitting of triplet O_2 by the singlet P_2 core in **2** may involve a single-electron transfer mechanism.[22] Indeed, single-electron oxidation has been reported for carbene-stabilized P_2 molecules (including **2**).[25]

Colorless X-ray quality crystals of **3** were obtained by recrystallization in toluene (under an oxygen- and water-free argon atmosphere). However, crystals of $\mathbf{3}\cdot(H_2O)_2$ were obtained when the recrystallization proceeded in air. While N_2O_4 exists in an equilibrium mixture of NO_2 at 25 °C (dissociation energy of N_2O_4: 14 kcal/mol),[1] compound **3** is sufficiently stable such that dissociation to L:PO_2 was not observed (dissociation energy of **3**: 49 kcal/mol).[17] It is noteworthy that the synthesis of **3** is extremely moisture- and temperature-sensitive. Improving the anhydrous nature of O_2 and conducting the preparation at low temperature effectively increases the yield of **3**.

Compound **3** was characterized by elemental analysis, infrared spectroscopy, ^{1}H, ^{13}C, ^{31}P NMR, and single-crystal X-ray diffraction.[16] The imidazole ^{1}H NMR resonance of **3** shifts to 6.25 ppm from 5.98 ppm for **2**.[14] Meanwhile, the ^{1}H-coupled ^{31}P NMR singlet resonance of **3** dramatically shifts downfield to 5.8 ppm from −52.4 ppm for **2**,[14] which is due to the electronegative oxygen atoms in **3** attracting the electron density away from the central phosphorus atoms. The infrared (IR) spectrum of **3** exhibits two characteristic PO_2 stretching frequencies at 1279 cm^{-1} (antisymmetric mode) and 1061 cm^{-1} (symmetric mode), which compare well to the computed frequencies (1290 cm^{-1} and 1061 cm^{-1}) of PO_2 in **3** (C_i symmetry), respectively.[17] Notably, due to the intermolecular hydrogen bonds involving the lattice water and the oxygen atoms of the $O_2P{-}PO_2$ core (Figure S1, Supporting Information [SI]), the stretching frequencies of PO_2 for $\mathbf{3}\cdot(H_2O)_2$ are red-shifted to 1269 cm^{-1} (antisymmetric mode) and 1057 cm^{-1} (symmetric mode).

The crystal structure of **3** reveals that this compound possesses C_i symmetry and contains an unprecedented $O_2P{-}PO_2$ core that adopts a trans-bent geometry due to the coordination of two bulky carbene ligands (Figure 1). It is instructive to delineate the structural effects of capping the diphosphorus core in **2** with four oxygen atoms. Each phosphorus atom in **3**, in the formal oxidation state of +4, is four-coordinate and resides in a distorted tetrahedral geometry, whereas each phosphorus atom in **2**, in the formal oxidation state of zero, is two-coordinate and adopts a bent geometry. The C(1)−P(1)−P(1A)−C(1A) torsion angles in both **2** and **3** are 180°.[14] The C(1)−P(1)−P(1A) bond angle [102.08(11)°] in **3** is only marginally less than that [103.19(6)°] in **2**. The P−P bond of **3** [2.310(2) Å] is about 0.1 Å longer than that in **2** [2.2052(10) Å] which, however, is almost the same as that [2.3103(7) Å] in a "Jack-in-the-Box" diphosphine.[26] The P−C bond distance [1.895(3) Å] in **3**, corresponding to the typical P−C single bond distance [i.e., the 1.871(11) Å P−C bond distance in **1**],[15] is about 0.13 Å longer than that [1.7504(17) Å] in **2**,[14] which may be attributed to the lack of P-to-C_{NHC} pπ back-donation in **3**. The P−O bond distances [1.466(3) and 1.470(3) Å] in **3** are comparable to the computed P−O bond distance (1.437 Å) in $O_2P{-}PO_2$ with D_{2d} symmetry,[6] the experimental P−O bond distances in L′:P(O)$_2$Cl [1.452(2) Å, L′: = :C{(*i*-Pr)NC(Me)}$_2$, **4**],[27] and in phosphine oxides (i.e., 1.48 Å for Ph_3PO).[28] In contrast, it is obviously shorter than the P−OH bond distance [1.5750(15) Å] in L′:P(O)$_2$OH[29] and the sum of phosphorus and oxygen covalent radii (1.73 Å),[30] suggesting the multiple-bond character of the phosphorus−oxygen bonds in **3**. The O−P−O bond angle [125.39(19)°] in **3** compares well to that [124.16(15)°] in **4**.[27]

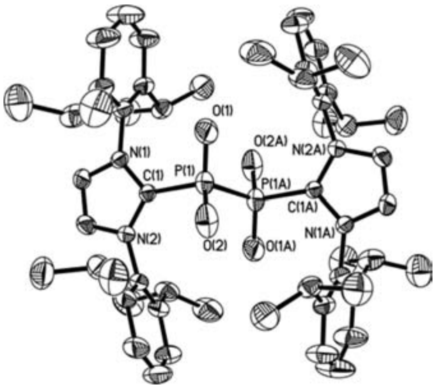

Figure 1. Molecular structure of L:(O)$_2$P−P(O)$_2$:L (L: = :C{N(2,6-$Pr^i_2C_6H_3$)CH}$_2$) (**3**) (thermal ellipsoids represent 30% probability; hydrogen atoms omitted for clarity). Selected bond distances (Å) and angles (deg). For **3**, P(1)−P(1A) 2.310(2), P(1)−C(1) 1.895(3), P(1)−O(1) 1.466(3), P(1)−O(2) 1.470(3), C(1)−P(1)−P(1A) 102.08(11), O(1)−P(1)−P(1A) 107.68(15), O(2)−P(1)−P(1A) 109.57(14), O(1)−P(1)−O(2) 125.39(19), O(1)−P(1)−C(1) 103.28(14), O(2)−P(1)−C(1) 106.27(15). For $\mathbf{3}\cdot(H_2O)_2$, P(1)−P(1A) 2.2132(13), P(1)−C(1) 1.876(2), P(1)−O(1) 1.458(2), P(1)−O(2) 1.467(2), C(1)−P(1)−P(1A) 102.51(8), O(1)−P(1)−P(1A) 109.42(11), O(2)−P(1)−P(1A) 109.55(11), O(1)−P(1)−O(2) 122.12(16), O(1)−P(1)−C(1) 105.65(11), O(2)−P(1)−C(1) 105.68(11).

In the crystal of $\mathbf{3}\cdot(H_2O)_2$[16] molecule **3** (also with C_i symmetry) exhibits somewhat different structural parameters (Figure 1, caption). This may be due to the packing effects and the hydrogen bonding interactions between lattice water molecules and **3** (Figure S1 in SI). Notably, the P−P bond [2.2132(13) Å] for $\mathbf{3}\cdot(H_2O)_2$ is about 0.1 Å shorter than that [2.310(2) Å] of the nonsolvated **3**, which indicates the flexibility of the P−P bond of compound **3**. The P−O bond distances [1.458(2) and 1.467(2) Å] in $\mathbf{3}\cdot(H_2O)_2$, however, are only little bit shorter than those in the nonsolvated **3** [1.466(3) and 1.470(3) Å]. As shown in the space-filling model of $\mathbf{3}\cdot(H_2O)_2$ (Figure S1 in SI), the steric bulk of the carbene ligands can effectively shield the P_2O_4 core and only allow two lattice water molecules to achieve hydrogen bonds with two of the four oxygen atoms of **3**.

The nature of **3** was further probed by density functional theory (DFT) computations at the B3LYP/DZP level.[17] The optimized **3** in C_i symmetry (Figure S3 in SI) corresponds to a rotational transition state, which is only 2.9 kcal/mol higher in energy than the C_1 minimum (Figure S2 in SI) of **3**. The packing effects may play a contributing role in the C_i conformation experimentally observed in the solid state of **3**. The computed structural parameters (i.e., d_{P-P} = 2.231 Å, d_{P-O} = 1.501 Å, d_{P-C} = 1.928 Å, O−P−O bond angle =123.56°) of **3** (C_i symmetry) are comparable to the experimental results for both **3** and $\mathbf{3}\cdot(H_2O)_2$.[16]

The localized molecular orbitals (LMOs) of the simplified model **3-H** [L: = :C(NHCH)$_2$; optimized in C_i symmetry, Figure S4 in SI] are shown in Figure 2. Natural bond orbital (NBO) analysis shows that one lone pair orbital of oxygen has mainly *s*-character (65.4%, av.), while another two lone pair orbitals of oxygen are essentially pure *p*-character (99.6%, av), which are somewhat distorted toward phosphorus. The central

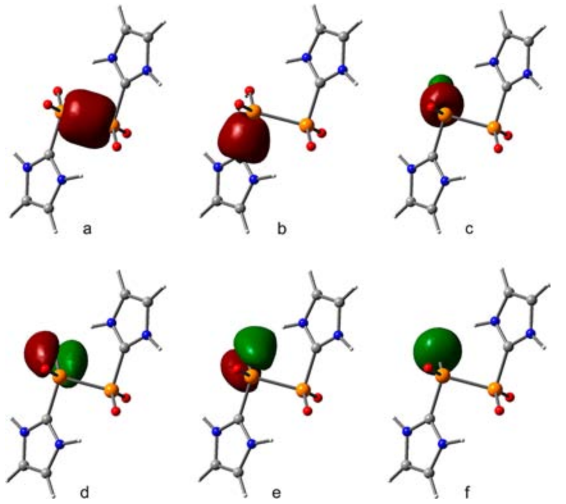

Figure 2. Localized molecular orbitals (LMOs) of **3-H** with C_i symmetry. (a) P−P σ-bonding orbital; (b) P−C σ-bonding orbital; (c) P−O σ-bonding orbital; (d, e, f) lone pair orbitals of O.

P−P bond in **3-H** has mainly *p*-character (22% *s*, 76% *p*, 2% *d*). The Wiberg bond indices (WBIs) (P−P, 0.673; P−C, 0.678) of **3-H** are lower than those (P−P, 1.004; P−C, 1.397) for **2**, indicating relatively weak P−P and P−C bonds in **3-H**. The P−O σ-bond polarization is 75% toward oxygen and 25% toward phosphorus. The WBI values of the P−O bonds (1.14, av) in **3-H** suggest modest multiple bond character of the P−O bonds. For the PO_2 unit in **3-H** phosphorus bears +1.8 positive charge, while each oxygen bears −1.1 negative charge. When considering the experimental data and theoretical analysis, two extreme resonance forms (**3A** and **3B**) may be proposed for **3** (Scheme 2, R = 2,6-$Pr^i_2C_6H_3$).

Scheme 2. Two Contributing Canonical Resonance Structures of 3

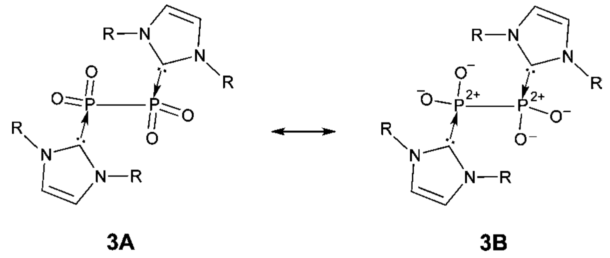

The synthesis of **3** through splitting molecular oxygen by carbene-stabilized P_2 suggests a new strategy to probe the exciting chemistry of highly reactive phosphorus oxides.

■ ASSOCIATED CONTENT

Ⓢ Supporting Information

Complete refs 17a and 17b, full details of the syntheses, computations, and X-ray crystal determination, including cif files. This material is available free of charge via the Internet at http://pubs.acs.org.

■ AUTHOR INFORMATION

Corresponding Author

robinson@uga.edu

Notes

The authors declare no competing financial interest.

■ ACKNOWLEDGMENTS

We are grateful to the National Science Foundation for support: CHE-1265212 (G.H.R., Y.W.), CHE-1057466 (P.v.R.S.), and CHE-1054286 (H.F.S.).

■ REFERENCES

(1) Cotton, F. A.; Wilkinson, G.; Bochmann, M.; Murillo, C. *Advanced Inorganic Chemistry*; 6th ed.; Wiley: New York, 1998.

(2) Schlesinger, R. B. In *Environmental Toxicants: Human Exposures and Their Health Effects*; 3rd ed.; Lippmann, M., Ed.; John Wiley & Sons, Inc.,: Hoboken, NJ, 2008.

(3) Mielke, Z.; McCluskey, M.; Andrews, L. *Chem. Phys. Lett.* **1990**, *165*, 146.

(4) Scherer, O. J.; Braun, J.; Walther, P.; Heckmann, G.; Wolmershaeuser, G. *Angew. Chem., Int. Ed. Engl.* **1991**, *30*, 852.

(5) Scherer, O. J.; Weigel, S.; Wolmershauser, G. *Angew. Chem., Int. Ed.* **1999**, *38*, 3688.

(6) Lohr, L. L., Jr. *J. Phys. Chem.* **1990**, *94*, 1807.

(7) Bauschlicher, C. W., Jr.; Zhou, M.; Andrews, L. *J. Phys. Chem. A* **2000**, *104*, 3566−3571.

(8) Wang, Y.; Robinson, G. H. *Chem. Commun.* **2009**, 5201−5213.

(9) Wang, Y.; Robinson, G. H. *Inorg. Chem.* **2011**, *50*, 12326−12337.

(10) Wang, Y.; Robinson, G. H. *Dalton Trans.* **2012**, *41*, 337−345.

(11) Martin, D.; Soleilhavoup, M.; Bertrand, G. *Chem. Sci.* **2011**, *2*, 389−399.

(12) Martin, D.; Melaimi, M.; Soleilhavoup, M.; Bertrand, G. *Organometallics* **2011**, *30*, 5304−5313.

(13) Wilson, D. J. D.; Dutton, J. L. *Chem.—Eur. J.* **2013**, *19*, 13626−13637.

(14) Wang, Y.; Xie, Y.; Wei, P.; King, R. B.; Schaefer, H. F., III; Schleyer, P. v. R.; Robinson, G. H. *J. Am. Chem. Soc.* **2008**, *130*, 14970−14971.

(15) Wang, Y.; Xie, Y.; Abraham, M. Y.; Gilliard, R. J., Jr.; Wei, P.; Schaefer, H. F., III; Schleyer, P. v. R.; Robinson, G. H. *Organometallics* **2010**, *29*, 4778−4780.

(16) See the SI for synthetic and crystallographic details.

(17) (a) Computations: The structures of **5** and the simplified **5-H** were optimized at the B3LYP/DZP DFT level with the *Gaussian 94* and *Gaussian 03* programs: Frisch, M. J.; et al. *Gaussian 94*, Revision B.3; Gaussian Inc.: Pittsburgh, PA, 1995; (b) *Gaussian 03*, revision C.02; Gaussian, Inc.: Wallingford, CT, 2004. Computional details can be found in the SI.

(18) Riess, J. G.; Van Wazer, J. R. *J. Am. Chem. Soc.* **1966**, *88*, 2166−2170.

(19) Walker, M. L.; Mills, J. L. *Inorg. Chem.* **1975**, *14*, 2438−2440.

(20) Riess, J. G.; Van Wazer, J. R. *J. Am. Chem. Soc.* **1967**, *89*, 851−856.

(21) Tellenbach, A.; Jansen, M. *Eur. J. Inorg. Chem.* **2003**, 3759−3766.

(22) Borovik, A. S.; Zinn, P. J.; Zart, M. K. In *Activation of Small Molecules: Organometallic and Bioinorganic Perspectives*; Tolman, W. B., Ed.; Wiley-VCH: Weinheim, Germany, 2006, p 187.

(23) Shah, S.; Protasiewicz, J. D. *Coord. Chem. Rev.* **2000**, *210*, 181−201.

(24) Xiong, Y.; Yao, S.; Mueller, R.; Kaupp, M.; Driess, M. *Nat. Chem.* **2010**, *2*, 577−580.

(25) Back, O.; Donnadieu, B.; Parameswaran, P.; Frenking, G.; Bertrand, G. *Nat. Chem.* **2010**, *2*, 369−373.

(26) Hinchley, S. L.; Morrison, C. A.; Rankin, D. W. H.; Macdonald, C. L. B.; Wiacek, R. J.; Cowley, A. H.; Lappert, M. F.; Gundersen, G.; Clyburne, J. A. C.; Power, P. P. *Chem. Commun.* **2000**, 2045−2046.

(27) Kuhn, N.; Stroebele, M.; Walker, M. *Z. Anorg. Allg. Chem.* **2003**, *629*, 180−181.

(28) Goggin, P. L. In *Comprehensive Coordination Chemistry*; Wilkinson, G., Gillard, R. D., McCleverty, J. A., Eds.; Pergamon: Oxford, U.K., 1987; Vol. 2.

(29) Kuhn, N.; Eichele, K.; Walker, M.; Berends, T.; Minkwitz, R. *Z. Anorg. Allg. Chem.* **2002**, *628*, 2026−2032.

(30) Cordero, B.; Gomez, V.; Platero-Prats, A. E.; Reves, M.; Echeverria, J.; Cremades, E.; Barragan, F.; Alvarez, S. *Dalton Trans.* **2008**, 2832−2838.